17-Beta-Estradiol Analog Inhibits Cell Proliferation by Induction of Apoptosis in Breast Cell Lines

MICHELLE HELEN VISAGIE,[1] LYNN-MARIE BIRKHOLTZ,[2] AND ANNA MARGARETHA JOUBERT[1]*
[1]*Department of Physiology, University of Pretoria, Arcadia 0007, South Africa*
[2]*Department of Biochemistry, University of Pretoria, Pretoria 0028, South Africa*

KEY WORDS antimitotic; tumorigenic; non-tumorigenic

ABSTRACT Microtubules are important targets when studying potential anticancer agents since disturbance of these microtubule dynamics results in cell cycle arrest and cell death. 2-Methoxyestradiol is a naturally occurring metabolite that exerts antiproliferative activity and induces apoptosis. Due to limited biological accessibly and rapid metabolic degradation, several analogs were synthesized. This study investigated the antiproliferative influence of an 2-methoxyestradiol analog, (8R, 13S, 14S, 17S)-2-Ethyl-13-methyl-7, 8, 9, 11, 12,13, 14, 15, 16, 17-decahydro-6H-cyclopenta[a]phenanthrane-3, 17-diyl bis(sulfamate) (EMBS) on cell proliferation, morphology and apoptosis induction in a estrogen receptor-positive breast adenocarcinoma cells line (MCF-7), estrogen receptor-negative highly metastatic breast cell line (MDA-MB-231) and a non-tumorigenic breast epithelial cell line (MCF-12A). Spectrophotometry results indicated that EMBS exerted differential antiproliferative activity in the three cell lines. Cell growth of the breast adenocarcinoma and highly metastatic breast cell line reached a plateau effect at 0.4 μM after 24 h of exposure. Light microscopy and polarization-optical transmitted light differential interference contrast demonstrated compromised cell density, cells blocked in metaphase and the presence of apoptotic characteristics after EMBS exposure for 24 h in all three cell lines. Transmission electron microscopy and scanning electron microscopy revealed hallmarks of apoptosis namely the presence of apoptotic bodies, shrunken cells and cell debris in EMBS-exposed cells. This investigation demonstrated that EMBS does exert antimitotic activity and induces apoptosis contributing to elucidating the signal transduction of EMBS in tumorigenic and non-tumorigenic breast cell lines. Findings warrant in-depth analysis of specific targets in vitro and subsequent in vivo investigation for anticancer therapy. *Microsc. Res. Tech. 00:000–000, 2014.*

INTRODUCTION

Tumorigenic cells demonstrate transformation in morphological- and growth-related properties including cell motility, shape, and hyperproliferation. The latter is due to abnormal assembly of microtubules and microfilaments since these cytoskeletal components regulate cell motility, anchorage-dependent growth and cell surface proteins (Brinkley et al., 1980). It has been hypothesized that these manifestations are a result of centromeres amplification and subsequent abnormal segregation leading to increased frequency of abnormal mitosis and chromosomal missegregation (Lingle et al., 2001). The exact symmetrical microtubule organization during cell division is essential and some chemotherapeutic agents are therefore targeted at disrupting the microtubule dynamics for induction of cell cycle arrest and ultimately cell death (Ecsedy et al., 2012; Leslie et al., 2010). A naturally occurring estradiol metabolite namely 2-methoxyestradiol exerts antimitotic activity due to its ability to bind to the colchicine binding site of β-tubulin (Stander et al., 2011b). 2-Methoxyestradiol failed to advance to United States Food and Drug Administration approval because of its low bioavailability and rapid metabolic breakdown (Visagie et al., 2012). Several newly developed 2-methoxyestradiol analogs have been designed and developed in recent years with improved bioavailability in our laboratory (Stander et al., 2011a, b).

The structure–activity relationship (SAR) pertaining to (8R, 13S, 14S, 17S)-2-Ethyl-13-methyl-7, 8, 9, 11, 12, 13, 14, 15, 16, 17-decahydro-6H-cyclopenta[a]-phenanthrane-3, 17-diyl bis(sulfamate) (EMBS) predicts potent anticancer activity with dual activity targeting proliferation and angiogenesis with increased bioavailability (Fig. 1) (Leese et al., 2008). Improved bioavailability is a result of the sulfamate groups that block inactivation of metabolism and deactivating conjugation and interaction with carbonic anhydrase. This characteristic causes reduction of first pass liver metabolism by sequestering the sulfates in red blood cells (Stander et al., 2011a, b). Moreover,

*Correspondence to: Anna Margaretha Joubert; Department of Physiology, University of Pretoria, Bag X 323, Arcadia 0007, South Africa.
E-mail: annie.joubert@up.ac.za

Received 29 October 2014; accepted in revised form 6 January 2014
REVIEW EDITOR: Prof. George Perry
Contract grant sponsor: Cancer Association of South Africa; The Struwig Germeshuysen Trust; Research Committee; School of Medicine; University of Pretoria; National Research Foundation and The Medical Research Council.
DOI 10.1002/jemt.22334
Published online 00 Month 2014 in Wiley Online Library (wileyonlinelibrary.com).

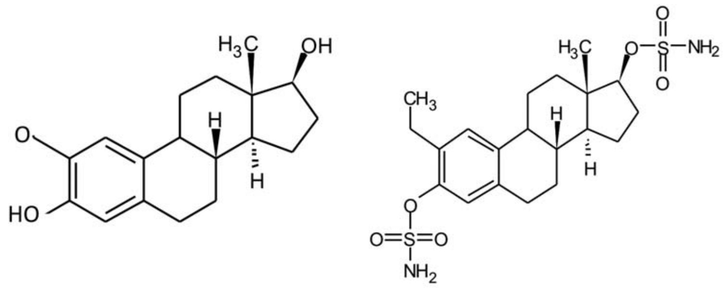

2-Methoxyestradiol

(8R, 13S, 14S, 17S)-2-Ethyl-13-methyl-7, 8, 9, 11, 12,13, 14, 15, 16, 17-decahydro-6H-cyclopenta[*a*]phenanthrane-3, 17-diyl bis(sulphamate) (EMBS)

Fig. 1. Structural differences between 2-methoxyestradiol and EMBS.

these sulfamate groups are reversible inhibitors of steroid sulfatase (Jourdan et al., 2010). In addition, the C-17 sulfamate substitution was documented to enhance antitumor activity in vitro and in vivo, where 2-ethyl estradiol analogs were reported to induce cell cycle arrest and apoptosis (Bupert et al., 2007; Foster et al., 2008; Jourdan et al., 2010; Wang et al., 2009). Even though these compounds are derivatives of estradiol they are independent of estrogen receptors and are not substrates for the P-glycoprotein pump and are thus active against taxanes-resistant tumors (Jourdan et al., 2010)..

It has been reported that EMBS exerts antiproliferative and antimitotic activity in an array of breast, prostate and ovarian tumorigenic cell lines (Bupert et al., 2007). In addition EMBS inhibited tumor growths in xenografts derived from estrogen receptor negative breast tumorigenic cells (MDA-MB-231) in female athymic nude mice and xenografts derived from prostate cancer cells (DU145) in male athymic nude mice using various doses including 60 mg/kg (once a day for 28 days), 90 mg/kg (three times a week), and 200 mg/kg (once a day) (Foster et al., 2008; Wang et al, 2009).

This study reported the influence of a 17-beta-estradiol analog as a potential anticancer agent in an estrogen-receptor positive breast adenocarcinoma cell line (MCF-7), a triple negative metastatic breast cell line (MDA-MB-231) and a non-tumorigenic breast epithelial cell line (MCF12A).

MATERIALS AND METHODS

Materials

Cell Lines. The MCF-7 cell line is an estrogen receptor-positive tumorigenic adherent breast epithelial cell line derived from metastatic sites in adenocarcinoma (Visagie et al., 2012). MCF-7 cells were supplied by Highveld Biological (Sandringham, South Africa.

MDA-MB-231 is an estrogen receptor-negative tumorigenic metastatic breast cell line and is commercially available from Microsep (Johannesburg, South Africa) (Visagie et al., 2012). Cells were grown and maintained in sterile 25 cm^2 tissue culture flasks at a humidified atmosphere at 37°C and 5% CO_2. Growth medium consisted of Dulbecco's Minimum Essential Medium Eagle (DMEM) supplemented with 10% heat-inactivated fetal calf serum (FCS) (56°C, 30min), 100 U/mL penicillin G, 100 μg/mL streptomycin and fungizone (250 μg/L). MCF-12A cells are non-tumorigenic transformed adherent human breast epithelial cells. These cells are produced by long-term cultures and form domes in confluent cultures (Visagie et al., 2012). The MCF-12A cells were a gift from Professor Parker (Department of Medical Biochemistry, University of Cape Town, South Africa). MCF-12A cells were cultured in growth medium consisting of a 1:1 mixture of Dulbecco's minimum essential medium eagle (DMEM) and Ham's-F12 medium, 20 ng/mL epidermal growth factor, 100 ng/mL cholera toxin, 10 μg/mL insulin and 500 ng/mL hydrocortisone, supplemented with 10% heat-inactivated FCS (56°C, 30 min), 100 U/mL penicillin G, 100 μg/mL streptomycin, and fungizone (250 μg/L).

Reagents. All required reagents of cell culture analytical grade were purchased from Sigma (St. Louis, United States of America) unless otherwise specified. Heat-inactivated FCS, sterile cell culture flasks, and plates were purchased from Sterilab Services (Kempton Park, Johannesburg, South Africa). Penicillin, streptomycin and fungizone were obtained from Highveld Biological (Sandringham, South Africa).

EMBS was synthesized by iThemba Pharmaceuticals (Modderfontein, Gauteng, South Africa), since this compound is commercially unavailable (Stander et al., 2011a). A stock solution of EMBS dissolved in dimethyl sulfoxide (DMSO) was prepared with a concentration of 10 mM and was stored at 4°C. The vehicle control sample composed of DMSO and growth medium where the DMSO content of the final dilutions never exceeded 0.05% (v/v).

Methods

Cell number determination. Crystal violet staining was used to demonstrate proliferative- and antiproliferative activity by staining deoxyribonucleic acid (DNA) (Visagie et al., 2012). Gillies et al. (1986) performed crystal violet staining to quantify cell number in monolayer cultures as a function of the absorbance of the dye taken up by the cells (Gillies et al., 1986). A dose-dependent study was chosen with a concentration range 0.2–1 μM, since it was previously established in our laboratory that this concentration series exerts antiproliferative activity. Exponentially growing MCF-7, MDA-MB-231, and MCF-12A cells were seeded in 96-well tissue culture plates at a cell density of 5,000 cells per well with an overnight attachment policy at 37°C in a humidified atmosphere containing 5% CO_2. To determine the starting number of cells, a baseline was established prior to exposure. Subsequently, the medium was discarded and cells were exposed to the EMBS at a concentration series of 0.1–1 μM for the 24 h since previous studies has demonstrated estradiol derivatives exerting antiproliferative activity in this concentration range (Visagie et al., 2012). Vehicle-treated controls were also included. Cells were fixed with 100 μL of 1% gluteraldehyde (incubation for 15 min at room temperature). Gluteraldehyde was discarded and cells were stained using 100 μL 0.1% crystal violet (incubated at room temperature for 30 min). Crystal violet was discarded and the 96-well plate was submersed under running water. Cells were solubilized using 200 μL 0.2% triton X-100 and incubated at room temperature for 30 min. Solution (100 μL) was transferred to a new microtitre plate. Afterward, the absorbance was determined at 570 nm using an EL_x800 Universal Microplate Reader available from Bio-Tek Instruments (Vermont, United States of America).

Morphology

Polarization-optical transmitted light differential interference contrast. Polarization-optical transmitted light differential interference contrast (PlasDIC) is a contrast method used to view morphology in a three-dimensional capacity (Visagie et al., 2012). PlasDIC displays the required phase profile which is relative to the product of the section thickness and the refractive index difference between the environment and the average refractive index of quartz. PlasDIC has high-quality DIC imaging of individual cells, cell clusters and thick individual cells in plastic cell-culture vessels possible for the first time. Cells was photographed before and after 24 h of exposure to 0.4 μM EMBS (optimal concentration demonstrated using crystal violet staining since the plateau effect is reached) using the Axiovert 40 CFL microscope (Carl Zeiss, Goettingen, Germany).

Light microscopy. The effects on morphology after exposure to 0.4 μM EMBS for 24 h was demonstrated using light microscopy (hematoxylin and eosin staining). Since crystal violet staining indicated that 0.4 μM EMBS exposure for 24 h resulted in significant inhibition of proliferation, this dosage and exposure period was used in all subsequent experiments. Hematoxylin and eosin staining also permits the identification of different mitotic phases, interphase, as well as apoptotic and abnormal cells (Visagie, 2010b). Cells (300,000 per well) were seeded on sterile coverslips in six well plates and incubated overnight. Afterwards cells were exposed to 0.4 μM EMBS for 24 h. Coverslips were transferred to staining dishes and cells were fixed with Bouin's fixative for 30 min. Subsequently Bouin's fixative was discarded and 70% ethanol was added to the coverslips for 20 min at room temperature before they were rinsed with tap water for 2 min. Mayer's hematoxylin was added to the coverslips for 20 min. Coverslips were rinsed with tap water for 2 min. Afterwards, 70% ethanol was added to the coverslip; followed by 1% eosin for 5 min. Eosin was discarded and coverslips were consecutively rinsed twice for 5 min with 70%, 96%, 100%, and xylol. Coverslips were mounted on microscope slides with resin and left to dry. Images were obtained by means of a Zeiss Axiovert MRc microscope (Zeiss, Oberkochen, Germany). In addition, hematoxylin- and eosin-stained cells were used to determine mitotic indices. In addition, hematoxylin- and eosin-stained samples were used to determine mitotic indices. Quantitative data for the mitotic indices were acquired by counting 1,000 cells for each sample ($n = 3$). Data expressed the average percentage of cells in interphase, prophase, anaphase, and telophase. Percentages of cells blocked in metaphase culminating in hallmarks of apoptosis were combined (Van Zijl et al., 2008). This hematoxylin and eosin staining yielded both qualitative and quantitative information.

Transmission electron microscopy. The in vitro influence of EMBS on interior cell morphology was visualized by means of transmission electron microscopy (TEM). Cells were fixed in 2.5% glutaraldehyde-formaldehyde mix and then with 0.5% osmium tetroxide. After each fixation step the samples were rinsed three times in 0.0075 M sodium phosphate buffer (pH 7.4). Samples were dehydrated using increasing concentrations of ethanol (30%, 50%, 70%, 90%, and 3× 100%) and embedded in quetol resin, sectioned with a microtome and placed on copper discs. Sections were contrasted with 4% aqueous uranyl acetate and Reynolds' lead citrate and viewed with a JOEL JEM 2100F transmission electron microscope (Electron Microscopy Unit, University of Pretoria, South Africa).

Scanning electron microscopy. Scanning electron microscopy (SEM) was used demonstrate the effects after exposure to 0.4 μM EMBS for 24 h on external cell morphology. MCF-7, MDA-231 and MCF-12A cells was seeded at 200,000 cells per well on heat-sterilized coverslips in 24-well plates. After 24 h attachment, the cells were exposed to 0.4 μM EMBS and incubated for 24 h. Cells were fixed by placing samples in 2.5 gluteraldehyde in 1.15 M Na^+/K^+ buffer for 1 h. Samples were rinsed thrice in 0.15 M Na^+/K^+ buffer and immersed in osmium tetroxide for 30 min. Subsequently samples were rinsed thrice in 0.15 M Na^+/K^+ buffer, followed by a graded dehydration in ethanol from 30% to 100%. Samples were covered in hexamethyldisilazane, left to dry in a dessicator overnight, sputter-coated in gold and viewed under a JSM 840 Scanning Electron Microscope (JEOUL, Tokyo, Japan).

Statistical Analysis

Qualitative data were collected from PLASDIC, light microscopy (hematoxylin and eosin staining), TEM, and SEM. Quantitative data were provided by means of crystal violet staining and mitotic indices provided by the hematoxylin and eosin staining. Quantitative data for the mitotic indices were acquired by counting 1,000 cells on each slide of the biological replicates and expressing the data as the percentage of cells in each phase of mitosis (prophase, metaphase, anaphase, and telophase), cells in interphase and cell demonstrating hallmarks of apoptosis. Data were statistically analyzed for significance using the analysis of variance-single factor model followed by a two-tailed Student's t test. Means are presented in bar charts, with T-bars referring to standard deviations. P values <0.05 were regarded as statistically significant.

RESULTS

Cell Number Determination

Spectrophotometry results of crystal violet staining indicated a concentration-dependent reduction in cell proliferation in all three cell lines (Fig. 2). Exposure to 0.4 μM for 24 h resulted in 40–35% growth inhibition in all three cell lines. However, this inhibition of cell proliferation reached a plateau effect in the tumorigenic cell lines. Thus, for all subsequent experiments, cell lines were exposed to 0.4 μM EMBS for 24 h to determine the effect on morphology and induction of autophagy, as well as apoptosis.

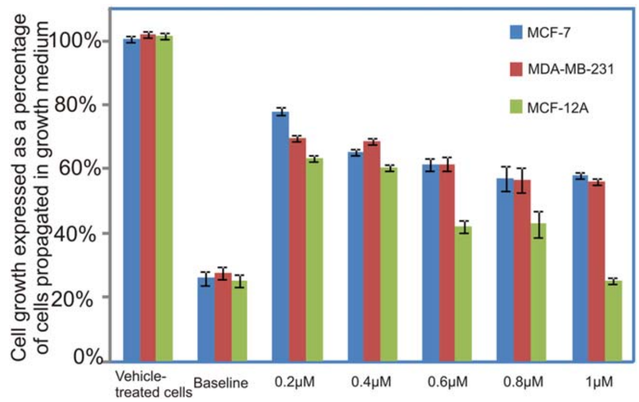

Fig. 2. Cell number determination by means of crystal violet staining of the estrogen receptor-positive adenocarcinoma MCF-7 cell line, estrogen receptor-negative metastatic MDA-MB-231 cell line and the non-tumorigenic MCF-12A cell line. EMBS exposure resulted in significant growth inhibition where a plateau was reached from 0.4 μM to 1 μM (40–35% growth inhibition) in the tumorigenic MCF-7 cell line and metastatic MDA-MB-231 cell line. In all subsequent experiments cell lines were exposed to 0.4 μM for 24 h. [Color figure can be viewed in the online issue, which is available at wileyonlinelibrary.com.]

Polarization-Optical Transmitted Light Differential Interference Contrast

Polarization-optical transmitted light differential interference contrast (PlasDIC) was employed to investigate the influence of 0.4 μM EMBS after 24 h of exposure on cell morphology (Fig. 3). All three cell lines revealed hallmarks of apoptosis. Decreased cell density, apoptotic bodies and cells blocked in metaphase were observed. All PlasDIC micrographs were taken at 10× magnification.

Light Microscopy

In order to support PLASDIC (qualitative) data, light microscopy utilizing hematoxylin and eosin staining was conducted to demonstrate the effects of 0.4 μM EMBS exposure for 24 h on cell density and morphology (Fig. 4). EMBS exposure resulted in decreased cell density, cells were blocked in metaphase and cell debris were observed when compared to vehicle-treated cells. Light microscopy micrographs were obtained at 40× magnification. Mitotic indices (quantitative data) revealed an increase in the number of apoptotic cells and an increase in the number of cells in metaphase in all three cell lines after exposure to 0.4 μM EMBS for 24 h (Table 1).

Transmission Electron Microscopy

TEM was conducted to visualize the interior of the cell after exposure to 0.4 μM EMBS for 24 h (Fig. 5). Apoptotic bodies, vacuoles and cell debris were present in the MCF-7 EMBS-treated cells, MCF-12A and MDA-MB-231 EMBS-treated cells.

Scanning Electron Microscopy

SEM was performed to demonstrate the effects of exposure to 0.4 μM EMBS for 24 h in all three cell lines (Fig. 6). SEM allows for investigation of the influence on morphology on the surface of cells. Cell debris, vacuole formation and apoptotic bodies were seen in the MCF-7 EMBS-treated cells, vacuole formation and cell debris in the MDA-MB-231 EMBS-treated cells and apoptotic bodies and cell debris in the MCF-12A EMBS-treated cells. In addition, all three treated cell lines possessed shrunken cells.

DISCUSSION

Several estrogen metabolites including 2-methoxyestradiol has been reported to exert antiproliferative- and antimitotic activity in recent years (Stander et al., 2011b; Visagie et al., 2011). However, 2-methoxyestradiol possesses poor bioavailability resulting in failure to advance to United States Food and Drug Administration approval (Visagie et al., 2012). The latter resulted in the in silico design and subsequent synthesis of several estradiol compounds (Stander et al., 2011a). This in vitro study demonstrated the influence of a 17-beta estradiol analog, EMBS, on cell growth, morphology and the induction of two types of cell death, namely apoptosis and autophagy on the estrogen receptor-positive breast adenocarcinoma MCF-7 cell line, the estrogen receptor-negative metastatic MDA-MB-231 cell line and the non-tumorigenic breast MCF-12A cell line.

Panchapakesan et al. (2011) reported that 2-substituted 17β-hydroxy/17-methylene estratrienes reduced cell growth in colon colorectal carcinoma cell line (HCT-116), large lung cancer cell line (NCIH-460), glioblastoma astrocytoma (U-251), and breast tumorigenic cell line (MDA-MB-435). In this investigation, proliferation studies indicated that EMBS exerts estrogen-independent antiproliferative activity in the tumorigenic MCF-7 cell line, metastatic MDA-MB-231 cell line, and the non-tumorigenic MCF-12A cell line. Furthermore, antiproliferative activity exerted by EMBS reached a plateau when exposed to 0.4 μM for 24 h. Studies conducted in our laboratory also demonstrated that other sulfamoylated estradiol analogs,

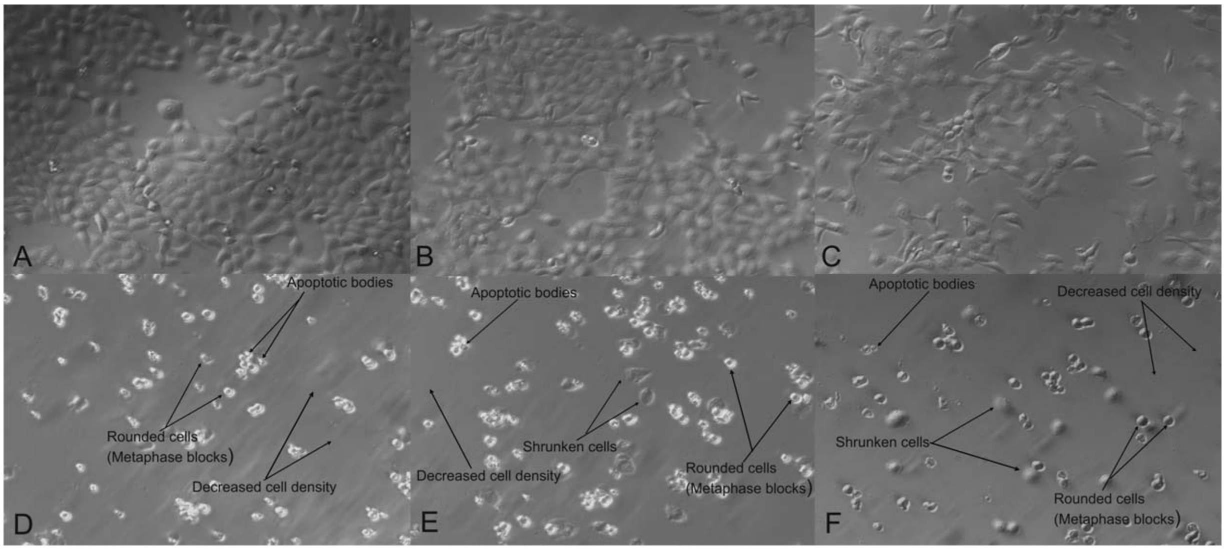

Fig. 3. PlasDIC micrographs of vehicle-treated MCF-7 cells (**A**), MDA-MB-231 cells (**B**), MCF-12A cells (**C**) EMBS-treated MCF-7 cells (**D**), EMBS-treated MDA-MB-231 cells (**E**), and EMBS-treated MCF-12A cells (**F**). Cells were exposed to 0.4μM of EMBS for 24 h. Vehicle-treated cells showed no abnormal morphology. EMBS-treated cells revealed decreased cell density, rounded cells (metaphase block), apoptotic bodies, and cell debris when compared to vehicle-treated cells (10× magnifcation).

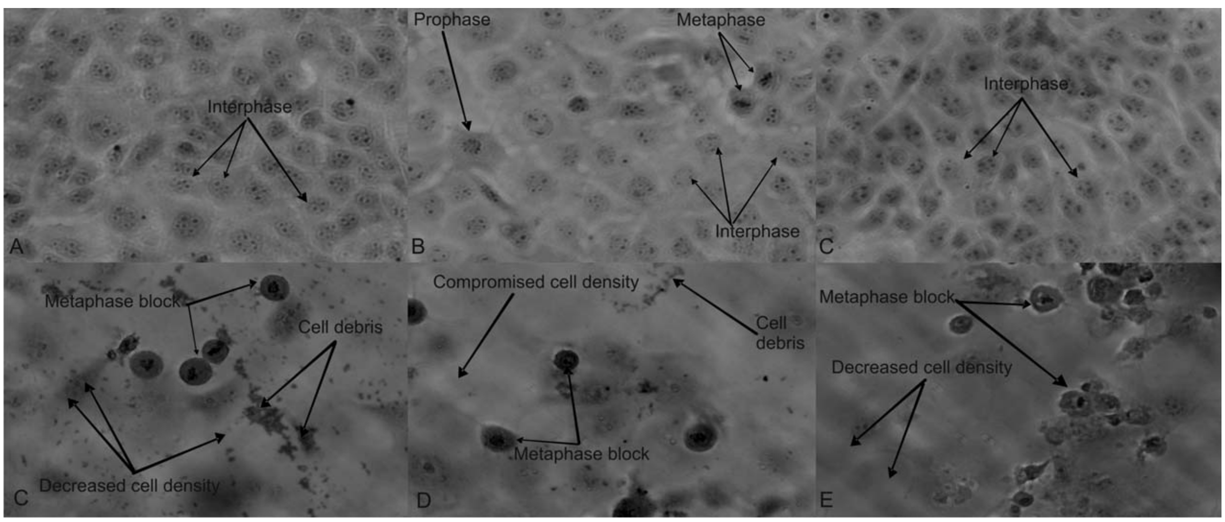

Fig. 4. Light microscopy of hematoxylin and eosin staining of MCF-7 vehicle-treated cells (**A**), MDA-MB-231 vehicle-treated cells (**B**), MCF-12A vehicle-treated cells (**C**), EMBS-treated MCF-7 cells (**D**), EMBS-treated MDA-MB-231 cells (**E**), and EMBS-treated MCF-12A cells (**F**). Cell lines treated with EMBS revealed decreased cell density and an increase number of cells present in metaphase when compared to vehicle-treated cells. In addition, apoptotic bodies, shrunken cells, and cell debris were observed (40× magnification).

TABLE 1. Percentage of cells in interphase, mitosis, and cells blocked in metaphase culminating in apoptosis

	Interphase	Prophase	Anaphase	Telophase	Cells blocked in metaphase culminating in apoptosis
MCF-7					
Vehicle-treated cells	96.1	1.3	0.8	0.8	1
EMBS-treated cells	55.6[a]	1.1	0.1	0.2	43[a]
MDA-MB-231					
Vehicle-treated cells	94.3	2.3	1.0	0.8	1.6
EMBS-treated cells	48.2[a]	1.9	0.7	0.3	48.9[a]
MCF-12A					
Vehicle-treated cells	95.5	2.2	0.9	0.2	1.2
EMBS-treated cells	54.7[a]	1.9	0.9	0.8	41.7[a]

Quantitative data for the mitotic indices were acquired by counting 1,000 cells for each sample (n = 3).
[a]Statistically significant P value of $<$0.05 when compared to vehicle-treated cells.

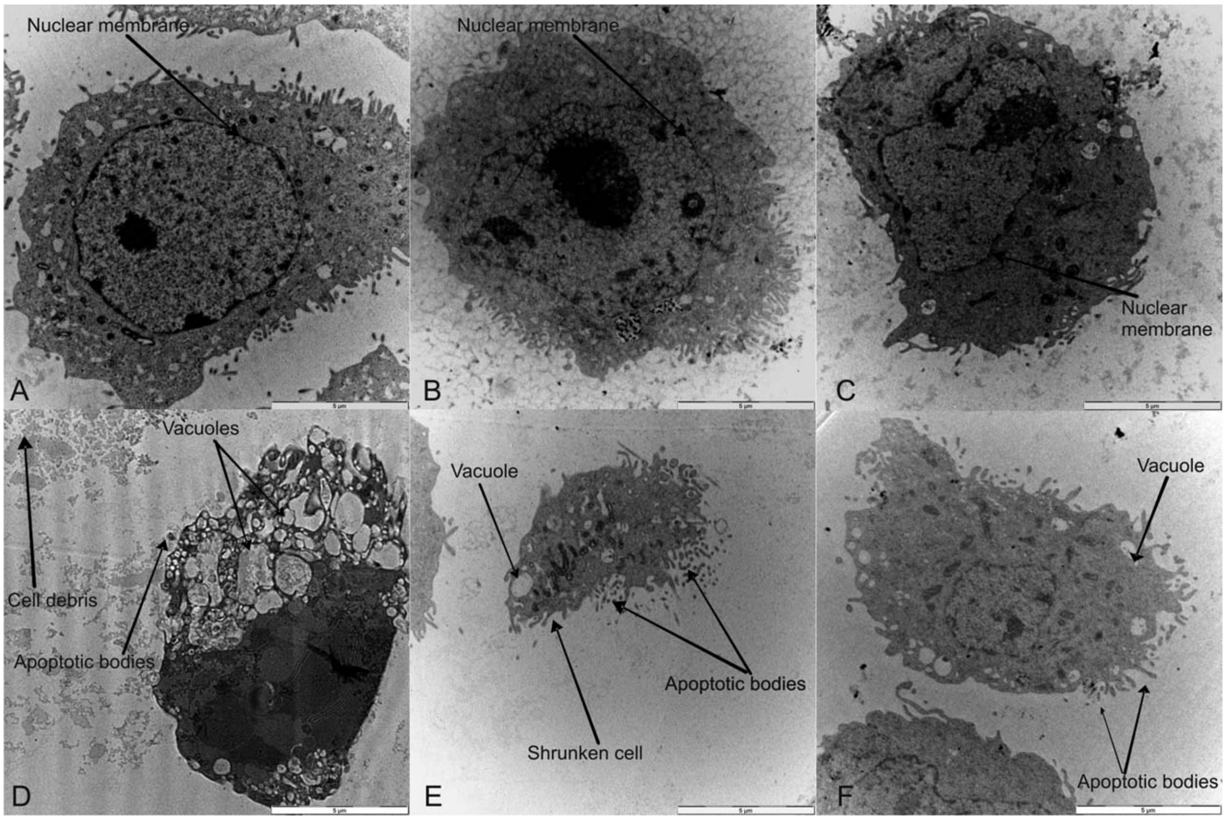

Fig. 5. Transmission electron microscopy of MCF-7 vehicle-treated cells (**A**), MDA-MB-231 vehicle-treated cells (**B**), MCF-12A vehicle-treated cells (**C**), EMBS-treated MCF-7 cells (**D**), EMBS-treated MDA-MB-231 cells (**E**), and EMBS-treated MCF-12A cells (**F**). Treated cell lines demonstrated the presence of apoptotic bodies and vacuoles when compared to vehicle-treated cells.

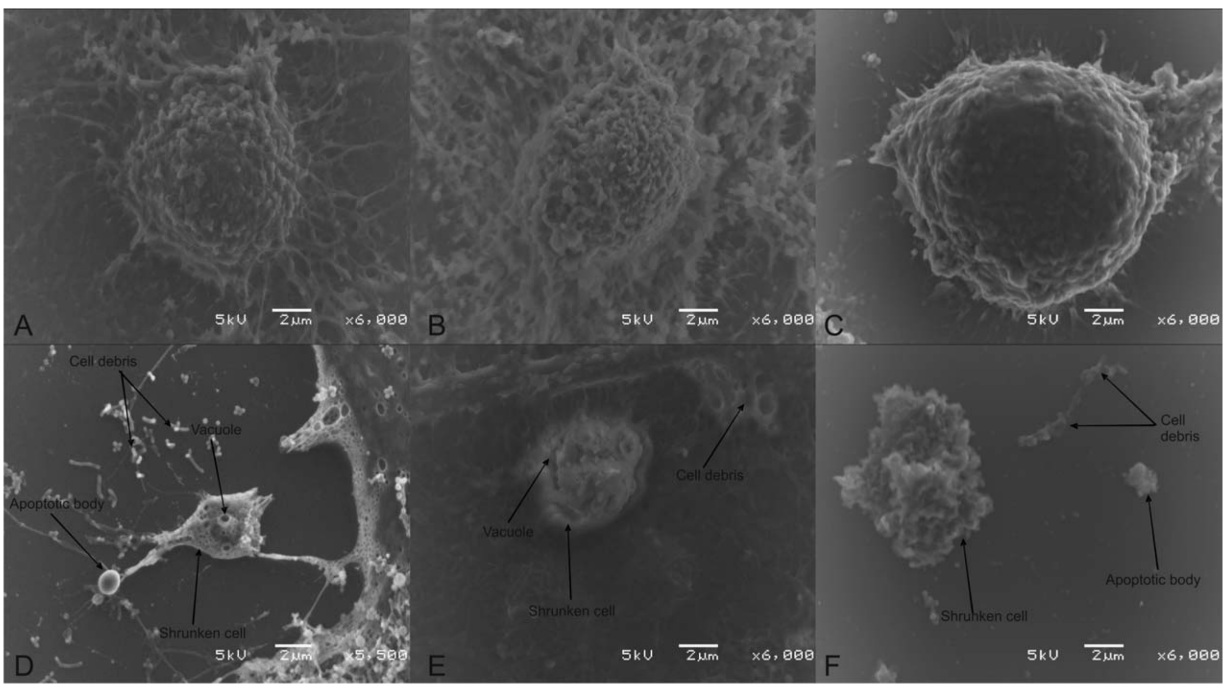

Fig. 6. Scanning electron microscopy of MCF-7 vehicle-treated cells (**A**), MDA-MB-231 vehicle-treated cells (**B**), MCF-12A vehicle-treated cells (**C**), EMBS-treated MCF-7 cells (**D**), EMBS-treated MDA-MB-231 cells (**E**), and EMBS-treated MCF-12A cells (**F**). Treated cells represented with shrunken cells and cell debris. Vacuole formation was observed in the MCF-7 and MDA-MB-231 cells when compared to vehicle-treated cells.

2-ethyl-3-*O*-sulfamoyl-estra-1,3,5(10),15-tetraen-17-ol, 2-ethyl-3-*O*-sulfamoyl-estra-1,3,5(10)16-tetraene, (8, 9, 13, 14, 17)-2-ethyl-17-hydroxy-13-methyl-7, 8, 9, 11, 12, 13, 14, 15, 16, 17-decahydro-6H-cyclopenta[*a*]phenanthren-3-yl sulfamate exert antiproliferation activity in a similar concentration range (Stander et al., 2011a, 2012, 2013).

Morphology findings include hallmarks of apoptosis namely apoptotic bodies, cell debris, shrunken cells and several cells blocked in metaphase after exposure to EMBS in all three cell lines. Bis-sulfamoylated 2-methoxyestradiol derivative, 2-methoxyestradiol-bis-sulfamate, induces apoptosis in several cell lines including MCF-7, breast adenocarcinoma cells (CAL51), prostate cancer cells (PC-3) and human umbilical vein endothelial cells (Newman et al., 2004, 2007; Visagie et al., 2010a,b, 2011; Wood et al. 2004). Sulfamoylated 2-methoxyestradiol analogs 2-ethyl-3-*O*-sulfamoyl-estra-1,3,5(10),15-tetraen-3-ol-17-one estronem and 2-ethyl-3-*O*-sulfamoyl-estra-1,3,5(10)16-tetraene also induced apoptosis in MDA-MB-231 cells (Stander et al., 2011). In addition, another 2-methoxyestradiol analog, 8R, 9S, 13S, 14S, 17S)−2-ethyl-17-hydroxy-13-methyl-7, 8, 9, 11, 12,13, 14, 15, 16, 17-decahydro-6H-cyclopenta[*a*]phenanthren-3-yl sulfamate induced apoptosis in MCF-7 cells, MDA-MB-231, and MCF-12A cells (Visagie et al., 2012). Furthermore, the promising antimitotic activity exerted by EMBS alluring as microtubule-targeted agent has been favored for decades. A microtubule-associated protein, tau, prominently found to be abnormally cleaved in Alzheimer's disease patients induced apoptosis in the human teratocarcinoma-derived cell line (NT2). Caspase 3 activity led to the release of the C-terminal of tau (19 amino acids) in vitro (Fasulo et al., 2002).

This study demonstrated that EMBS possess estrogen-independent antiproliferative and antimitotic activity and induces apoptosis in breast cell lines. However, this study also indicated that EMBS does not exert differential effects on tumorigenic and non-tumorigenic breast cell lines. Future studies will involve further investigation of the molecular mechanism utilized by EMBS and elucidating what structural alteration resulted in the loss of differential signaling between tumorigenic and non-tumorigenic cell lines.

REFERENCES

Brinkley BR, Beall PT, Wible LJ, Mace ML, Turner DS, Cailleau RM. 1980. Variations in cell form and cytoskeleton in human breast carcinoma cells in vitro. Cancer Res 40:3118–3129.

Bupert C, Leese MP, Mahon MF, Ferrandis E, Regis-Lydi S, Kasprzyk PG, Ho YT, Purohit A, Reed MJ, Potter BV. 2007. 3,17-Disubstituted 2-Alkylestra-1,3,5(10)-trien-3-ol derivatives: synthesis, in vitro and in vivo anticancer activity. J Med Chem 50:4431–4443.

Ecsedy JA, Manfredi M, Chakravarty A, D'Amore N. 2012. Current and next generation antimitotic therapies in cancer. In: Signaling and Pathways in Cancer Pathogonesis and Therapy. Frank DA, editor. Springer, New York, pp 5–21.

Fasulo L, Ugolini G, Visintin M, Bradcury A, Brancolini C, Verzillo V, Novak M, Cattaneo A. 2002. The neuronal microtubule-associated protein tau is a substrate for caspase 3 and an effector of apoptosis. J Neurochem 75:624–633.

Purohit A. 2008. 2-MeOE2bisMATE and 2-EtE2bisMATE induce cell cycle arrest and apoptosis in breast cancer xenografts as shown by a novel ex vivo technique. Breast Cancer Treat 111:251–260.

Gillies RJ, Didier N, Denton M. 1986. Determination of cell number in monolayer cultures. Anal Biochem 159:109–113.

Jourdan F, Leese MP, Dohle W, Hamel E, Ferrandism E, Newman SP, Purohit A, Rees MJ, Potter BVL. 2010. Synthesis, antitubulin, and antiproliferative SAR of analogues of 2-methoxyestradiol-3- 17-O, O-bis-sulfamate. J Med Chem 53:2942–2951.

Leese MP, Jourdan FL, Gaukroger K, Mahon MF, Newman SP, Foster PA, Stengel C, Regis-Lydi S, Di Fiore A, De Simone G, Supuran CT, Purohit A, Reed MJ, Potter BVL. 2008. Structure-activity relationship of C-17-substituted estratrienes as anticancer agents. J Med Chem 51:1295–1308.

Leslie BJ, Holadau CR, Ngugen T, Hergenrother PJ. 2010. Phenylcinn mides as novel antimitotic agents. J Med Chem 53:3964–3972.

Lingle WL, Barret SL, Negron VC, D'Assoro AB, Boeneman K, Liu W, Whirehead CM, Reynolds C, Salisbury JL. 2001. Centromere amplification drives chromosomal instability in breast tumor development. PNAS 99:1978–1983.

Newman SP, Foster PA, Ho YT, Day JM, Raibaikady B, Kasprzyk PG, Leese MP, Potter BV, Reed MJ, Purohit A. 2007. The therapeutic potential of a series of bioavailable anti-angiogenic microtubule disruptors as therapy for hormone-independent prostate and breast cancers. Br J Cancer 97:1673–1682.

Newman SP, Leese MP, Purohit A, James DRC, Rennie CE, Potter BVL. 2004. Inhibition of in vitro angiogenesis by 2-Methoxy- and 2-ethyl-estrogen sulfamates. Int J Cancer 109:533–540.

Panchapakesan G, Dhayalan V, Moorthy ND, Saranya N, Mohanakrishnan AK. 2011. Synthesis of 2-substitued 17β-hydroxy/17-methylene estratrienes and their in vitro cytotoxicity in human cancer cell cultures. Steroids 76:1491–1504.

Stander A, Joubert F, Joubert A. 2011a. Docking, synthesis, and in vitro evaluation of antimitotic estrone analogues. Chem Biol Drug Des 77:173–181.

Stander XX, Stander BA, Joubert AM. 2011b. In vitro effects of an in silico-modelled 17β-estradiol derivative in combination with dichloroacetic acid on MCF-7 and MCF-12A cells. Cell Prolif 44: 567–581.

Stander BA, Joubert F, Tu C, Sippel KH, McKenna R, Joubert AM. 2012. In vitro evaluation of ESE-15-ol, an estradiol analogue with nanomolar antimitotic and carbonic anhydrase inhibitory activity. Plos One 7:e52205.

Stander BA, Joubert F, Tu C, Sippel KH, McKenna R, Joubert AM. 2013. Signaling pathways of ESE-16, an antimitotic and anticarbonic anhydrase estradiol analog, in breast cancer cells. Plos One 8: e53853.

Van Zijl C, Lottering ML, Steffens F, Joubert A. 2008. In vitro effects of 2-methoxyestradiol on MCF-12A and MCF-7 cell growth, morphology and mitotic spindle formation. Cell Biochem Funct 26: 632–42.

Visagie MH, Joubert AM. 2010a. 2-Methoxyestradiol-bis-sulfamate induces apoptosis and autophagy in a tumorigenic breast epithelial cell line. Mol Cell Biochem 357:343–352.

Visagie MH, Joubert AM. 2010b. In vitro effects of 2-methoxyestradiol-bis-sulphamate on cell numbers, membrane integrity, morphology and possible induction of apoptosis and autophagy in a non-tumorigenic breast epithelial cell line. Cell Mol Biol Lett 15:564–581.

Visagie MH, Joubert AM. 2011. In vitro effects of 2-methoxyestradiol-bis-sulphamate on reactive oxygen species and possible apoptosis induction in a breast adenocarcinoma cell line. Cancer Cell Int 11: 43.

Visagie MH, Mqoco TV, Joubert AM. 2012. Sulphamoylated estradiol analogue induces antiproliferative activity and apoptosis in breast cell lines. Cell Mol Biol Lett 17:549–585.

Wang C, Youle RJ. 2009. The role of mitochondria in apoptosis. Annu Rev Genet 43:95–118.

Wood L, Leese MP, Mouzakiti A, Purohit A, Potter BV, Reed MJ, et al. 2004. 2-MeOE2bisMATE induces caspase-dependent apoptosis in CAL51 breast cancer cells and overcomes resistance to TRAIL via cooperative activation of caspases. Apoptosis 9:323–332.